

## Phorbol-12-myristate 13-Acetate Acting through Protein Kinase C $\epsilon$ Induces Translocator Protein (18-kDa) *Tspo* Gene Expression<sup>†</sup>

Amani Batarseh,<sup>‡,§</sup> Christoforos Giatzakis,<sup>‡</sup> and Vassilios Papadopoulos<sup>\*,‡,§</sup>

Department of Biochemistry & Molecular and Cell Biology, Georgetown University Medical Center, Washington, DC 20057, and The Research Institute of the McGill University Health Centre and the Department of Medicine, McGill University, 1650 Cedar Avenue, Montreal, Quebec H3G 1A4, Canada

Received July 6, 2008; Revised Manuscript Received September 3, 2008

**ABSTRACT:** Translocator protein (TSPO) is an 18-kDa cholesterol-binding protein that is expressed at high levels in steroid synthesizing and several cancer cells where it is involved in steroidogenesis and cell proliferation, respectively. The factors regulating *Tspo* expression are unknown. We analyzed *Tspo* transcriptional responses to the tumor promoter, phorbol-12-myristate 13-acetate (PMA), in cells with varying TSPO levels. PMA induced *Tspo* promoter activity and *Tspo* mRNA levels in TSPO-poor nonsteroidogenic cells (NIH-3T3 fibroblasts and COS-7 kidney) but not in TSPO-rich steroidogenic cells (MA-10 Leydig) with high basal *Tspo* transcriptional activity. The stimulatory effect of PMA was mediated by an 805–515-bp region upstream of the transcription start site. Electrophoretic mobility shift assay (EMSA) revealed that PMA induced binding of c-jun and GA-binding protein transcription factor (GABP- $\alpha$ ) to their respective activator protein 1 (AP1) and v-ets erythroblastosis virus E26 oncogene homologue (Ets) sites in this region. Protein kinase C (PKC)-specific inhibitors blocked PMA induction of *Tspo* promoter activity with an inhibition profile suggestive of involvement of PKC $\epsilon$ . PKC $\epsilon$  expression correlated with TSPO content in the three cell lines. In NIH-3T3 cells, PKC $\epsilon$  overexpression induced *Tspo* promoter activity and mRNA levels and enhanced PMA-induced up regulation of c-jun and TSPO. In MA-10 cells, a PKC $\epsilon$ -specific translocation inhibitor peptide reduced basal *Tspo* promoter activity. PKC $\epsilon$  siRNA pool reduced PKC $\epsilon$  and TSPO levels in MA-10 cells indicating a role for PKC $\epsilon$  in regulating TSPO expression. Taken together, these data suggest that elevated TSPO expression in steroidogenic cells may be due to high constitutive expression of PKC $\epsilon$  that renders them unresponsive to further induction while PMA activation of PKC $\epsilon$  drives inducible TSPO expression in nonsteroidogenic cells, likely through AP1 and Ets.

The translocator protein (18-kDa; TSPO)<sup>1</sup>, formerly known as the peripheral-type benzodiazepine receptor, is a high-affinity drug- and cholesterol-binding protein that was first identified in 1977 as an alternative binding site in the kidney for the benzodiazepine diazepam (1, 2). TSPO binds various classes of organic compounds, including isoquinoline carboxamides such as PK11195 (3). TSPO is found in most tissues, although its expression among each tissue varies considerably (1, 3, 4). Secretory and glandular tissues, especially steroid hormone producing cells, are particularly rich in TSPO (1). Intermediate levels of this protein are found

in renal and myocardial tissues, and lower levels are present in the brain and liver (1, 5). TSPO resides primarily in the outer mitochondrial membrane, where it regulates the transport of the steroid hormone precursor, cholesterol, to the inner mitochondrial membrane. This transport process is the rate-determining step in steroidogenesis (1). The ubiquitous expression of TSPO, taken with its ability to bind cholesterol with high affinity (1), suggests that, in non-steroidogenic cells, TSPO regulates mitochondrial cholesterol compartmentalization and membrane biogenesis, events critical for mitochondrial function and multiple cellular processes (1). Indeed, in addition to its well-established role in steroidogenesis, TSPO has been implicated in cellular respiration, oxidative processes, proliferation, and apoptosis (1, 3).

Compared to normal human tissues, cancerous tissues of the breast, ovary, colon, prostate, and liver contain elevated levels of TSPO, implying that TSPO may participate in carcinogenesis (6–10). The finding that TSPO expression is positively correlated with the metastatic potential of human breast and brain tumors supports this idea (1, 6–8). A number of physiological and pharmacological modulators have been shown to alter TSPO levels. These modulators include peroxisome proliferators, IL-1, ginkgolide B, TNF-

<sup>†</sup> This work was supported by Grant R01 ES07747 from the National Institutes of Health (to V.P.). V.P. was also supported by a Canada Research Chair in Biochemical Pharmacology. The Research Institute of MUHC is supported in part by a Center grant from Le Fonds de la recherche en santé du Québec.

\* To whom correspondence should be addressed. Telephone: 514-934-1934 ext. 44580. Fax: 514-934-8439. E-mail: vassilios.papadopoulos@mcgill.ca.

<sup>‡</sup> Georgetown University Medical Center.

<sup>§</sup> McGill University Health Centre.

<sup>1</sup> Abbreviations: AP1, activator protein 1; EMSA, electrophoretic mobility shift assay; Ets, v-ets erythroblastosis virus E26 oncogene homologue; GABP, GA binding protein transcription factor; PKC $\epsilon$ , protein kinase C epsilon; PMA, phorbol-12-myristate 13-acetate; Sp1, specificity protein 1/Sp1 transcription factor; TSPO, translocator protein (18-kDa).

Table 1: Oligonucleotide Sequences Used in Electrophoretic Mobility Shift Assays

oligonucleotide name	sequence
S-AP1 wt	CTCTAATTGACTCACAGGAAGAGGTT
AS-AP1 wt	AACCTCTTCCTGTGAGTCAATTAGAG
S-AP1 wt biotin5	CTCTAATTGACTCACAGGAAGAGGTT
AS-AP1 wt biotin5	AACCTCTTCCTGTGAGTCAATTAGAG
S-AP1 mut	CTCTAATTCTCTCACAGGAAGAGGTT
AS-AP1 mut	AACCTCTTCCTGTGAGAGAATTAGAG
S-Ets mut	CTCTAATTGACTCACAGTCAGAGGTT
AS-Ets mut	AACCTCTGACTGTGAGTCAATTAGAG

$\alpha$ , serotonin, norepinephrine, and dopamine (3, 4, 11). Among these, peroxisome proliferators and ginkgolide B have been shown to reduce *Tspo* gene transcription (12, 13).

Despite a wealth of data on TSPO expression, little is known about the mechanisms underlying the transcriptional regulation of *Tspo*. Sequence analysis of the mouse *Tspo* promoter revealed that this promoter lacks TATA and CCAAT elements but contains a series of proximal GC boxes. This promoter also harbored a number of putative binding sites for transcription factors such as v-ets erythroblastosis virus E26 oncogene homologue (Ets), AP1, specificity protein 1/specificity protein 3 (Sp1/Sp3), AP2, Ik2, GATA, SOX, and SRY (5). In an analysis of the mechanisms underlying differential *Tspo* transcription in TSPO-rich steroidogenic Leydig cells and nonsteroidogenic fibroblasts, two proximal Sp1/Sp3 sites and members of the Ets family of transcription factors were found to be important for basal transcriptional activity (5, 14). These studies demonstrated that separate regions of the promoter drive *Tspo* transcription in steroidogenic cells and nonsteroidogenic cells (5), suggesting that tissue-specific transcriptional regulation accounts for differences in TSPO expression between these cell types. However, the factors mediating the increased *Tspo* expression in steroidogenic and tumor cells remain unknown.

Phorbol esters such as phorbol-12-myristate 13-acetate (PMA) promote skin tumor formation, making them useful tools in experimental carcinogenesis studies (15). PMA activates several isoforms of protein kinase C (PKC). PKC is a critical component of signal transduction pathways engaged by diverse stimuli in a variety of cell types (16). The PKC family comprises 11 known serine-threonine protein kinase isoforms with different biological functions (17). These isoforms can be divided into three groups based on activation requirements. Conventional PKC isoenzymes ( $\alpha$ ,  $\beta$ I,  $\beta$ II,  $\gamma$ ) require phosphatidylserine, diacylglycerol, and  $\text{Ca}^{2+}$  for activation. The unconventional or typical isoforms ( $\delta$ ,  $\theta$ ,  $\epsilon$ ,  $\eta$ ) require phosphatidylserine and diacylglycerol but not  $\text{Ca}^{2+}$  for their activation. The atypical group ( $\xi$ ,  $\lambda$ ) requires only phosphatidylserine. PKC isoform expression and distribution is cell-type and condition-specific (18).

PKC isoforms participate in diverse biological processes including cell proliferation, differentiation, apoptosis, steroidogenesis, and carcinogenesis (19). PKC plays a critical role in steroid production through regulation of gene expression (20–22). In addition, several PKC isoforms participate in cancer development, formation, progression, suppression, and/or metastasis (19). PKC $\epsilon$ , in particular, has been shown to be involved in tumor cell invasion, metastasis, and recurrence (23), and it is abundant in endocrine, neuronal, and immune cells (23, 24). Here, we analyzed *Tspo* transcriptional responses in steroidogenic (MA-10 mouse

tumor Leydig cells) and nonsteroidogenic cells (NIH-3T3 mouse fibroblasts and SV-40 transformed COS-7 monkey kidney cells). Our data reveal that high levels of endogenous PKC $\epsilon$  regulate *Tspo* expression in TSPO-rich steroidogenic cells while PMA induces *Tspo* expression in TSPO-poor nonsteroidogenic cells, with PKC $\epsilon$  mediating this effect.

## MATERIALS AND METHODS

**Cell Culture.** MA-10 cells were a gift from Mario Ascoli (University of Iowa, Ames, IA). Cells were cultured in T75 cm<sup>2</sup>-cell culture flasks (Dow Corning Corp., Corning, NY) and grown in DMEM/Ham-F12 nutrient mixture (Sigma Chemical Co., St. Louis, MO) supplemented with 5% fetal bovine serum and 2.5% heat-inactivated horse serum (Life Technologies, Gaithersburg, MD). NIH-3T3 cells and SV40-transformed COS-7 monkey kidney cells (Lombardi Cancer Center Tissue Culture Facility, Washington, DC) were maintained in DMEM supplemented with 10% normal calf serum and fetal bovine serum, respectively. Before experimentation, MA-10, NIH-3T3, and COS-7 cells were allowed to recover from plating for 24 h.

**Determination of TSPO Levels.** TSPO levels were indirectly determined by measuring binding of [3H]PK 11195 [1-(2-chlorophenyl)-N-methyl-N-(1-methyl-propyl)-3-isoquinoline carboxamide] (SA, 85.5 Ci/mmol, NEN Life Science Products) to cellular protein extracts. The assay was performed as previously described (25). In brief, cells were scraped from 150 mm culture dishes into 5 mL of PBS, dispersed by trituration, and centrifuged at 1200g for 5 min. The cell pellets were resuspended in PBS, and binding studies were performed on 5  $\mu$ g of protein for MA-10 and 50  $\mu$ g for NIH-3T3 or COS-7 from the cell suspensions. After 120 min incubation, assays were stopped by filtration through Whatman GF/C filters and washed with 15 mL of ice-cold PBS. Radioactivity trapped on the filters was determined by liquid scintillation counting at 50% counting efficiency. The dissociation constant ( $K_d$ ) and the number of binding sites ( $B_{\text{max}}$ ) were determined by Scatchard plot analysis of the data using the LIGAND program (KBLL, version 4.0, Biosoft, Ferguson, MO).

**Immunoblotting.** MA-10, NIH-3T3, and COS-7 cells were lysed in cold RIPA buffer (Cell Signaling, Danvers, MA) supplemented with Halt protease inhibitor cocktail (Pierce, Rockford, IL). Protein was measured using a standard Bradford assay (Bio-Rad, Hercules, CA). Proteins (15  $\mu$ g) were electrophoresed on 4–12% tris-glycine polyacrylamide gels (Invitrogen), transferred onto nitrocellulose membranes, and probed with antibodies to PKC $\epsilon$  (sc-214, Santa Cruz, Biotechnology, Santa Cruz, CA), TSPO (26), c-jun (sc-44-g, Santa Cruz), p-c-jun (Ser73) (9164, Cell Signaling Technology, Danvers, MA), or GAPDH (Trevigen, Gaithersburg, MD). Immunoreactive proteins were then visualized by enhanced chemiluminescence (Amersham, Piscataway, NJ).

**Luciferase Reporter Constructs and in Vitro-Directed Mutagenesis.** A 2700-bp fragment of the *Tspo* promoter was cloned upstream of a firefly luciferase gene in pGL3-basic (pGL3-2700), and a series of 5' unidirectional deletions were made (pGL3-805, -585, -515, -301, -214, -123, and -15) as described previously (5). Plasmids with point mutations were generated using pGL3-805 as a template and by PCR with

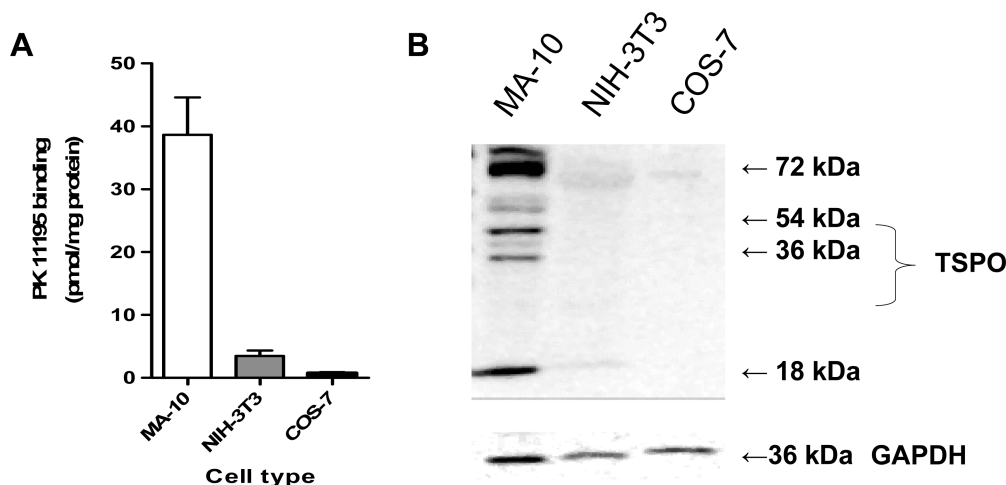


FIGURE 1: TSPO levels in MA-10, NIH-3T3, and COS-7 cells. (A) TSPO levels, as determined by [ $^3$ H]PK 11195 binding ( $B_{\max}$ ). Values are derived from three independent experiments ( $n = 9$ ). (B) Immunoblot analysis of TSPO. GAPDH served as a loading control. The gel is representative of three independent experiments.

overlapping primers containing the mutation (14). All plasmid sequences were verified through DNA sequencing.

**Transfection and Luciferase Assay.** MA-10, NIH-3T3, and COS-7 cells were seeded in 6-well plates at a density of 90 000 cells per well for MA-10 and NIH-3T3 and 150 000 for COS-7 cells per well. Transfection of reporter plasmids (1.5  $\mu$ g) was performed 24 h later using fuge6 (Roche, Indianapolis, IN) for MA-10 cells and polyfect (Qiagen, Valencia, CA) for NIH-3T3 and COS-7 cells. All cultures received equimolar amounts of experimental constructs, with PUC19 or empty vector being used to keep the final amount of DNA constant. All cultures were cotransfected with a *Renilla* luciferase reporter under the control of the thymidine kinase promoter (PRLTK, Promega Corp. Madison, WI) to normalize for transfection efficiency. Twenty-four hours after transfection, cells were treated with PMA (Sigma-Aldrich), dimethylsulfoxide (DMSO, vehicle) (Sigma-Aldrich), or 4 $\alpha$ -phorbol-12-myristate 13-acetate (4 $\alpha$ -PMA) (Promega Corp.) for 24 h or as otherwise indicated. Cellular extracts obtained with 1 $\times$  passive lysis buffer (Promega Corp.) were then processed with the dual-luciferase reporter system (Promega Corp.), and activity was measured using the Victor<sup>2</sup> automated plate reader (Perkin-Elmer, Waltham, MA).

**Quantitative Real Time (QRT)-PCR.** MA-10, NIH-3T3, and COS-7 cells ( $\sim 1 \times 10^6$ ) were seeded in 100 mm<sup>2</sup> plates and treated with DMSO or PMA 24 h later. RNA was extracted using the Rneasy Kit (Qiagen) according to the manufacturer's instructions. RNA (1  $\mu$ g) was reverse transcribed, and the resulting cDNA was used as a template for real time PCR using *Tspo* specific primers and SYBR GREEN dye. Mouse primers were used for MA-10 and NIH-3T3 cells. Primer sequences for amplification of COS-7 *Tspo* mRNA (forward, 5'-AGCCTGGGGTGCTTCGTG-3'; reverse, 5'-TGTCGGGCACCAAAGAAGAT-3') were designed from a region of the COS-7 *Tspo* promoter that was conserved with the human, cow, pig, mouse, and rat promoters. *Tspo* mRNA was quantified using the standard curve method. Amplification of 18s rRNA served as a control.

**Cell Proliferation Assay.** NIH-3T3 and COS-7 cells were seeded in 96-well plates at a density of 1000 cells/well, while MA-10 cells were plated at a density of 750 cells/well.

Cellular proliferation was determined by BrdU incorporation using a commercially available kit (Roche). BrdU labeling was performed according to the manufacturer's protocol using a labeling time of 6 h.

**Preparation of Nuclear Extracts and Electrophoretic Mobility Shift Assay (EMSA).** Nuclear extracts were prepared using NE-PER nuclear and cytosolic extraction reagents (Pierce Chemical Co., Rockford, IL). For EMSA, double-stranded, 5'-biotinylated oligonucleotides containing wild type and mutant AP1-binding sequences (Table 1) were incubated with 5  $\mu$ g of NIH/3T3 nuclear extracts. Unlabeled double-stranded AP1 and Ets oligonucleotides were used for competition experiments. EMSA was carried out using the LightShift chemiluminescent EMSA kit (Pierce Chemical Co.) in the presence of EDTA and Mg<sup>2+</sup>. The manufacturer's protocol was slightly modified to optimize protein-DNA interactions in the presence of antibodies. DNA-protein complexes were separated on 6% nondenaturing polyacrylamide gels, transferred to nylon membranes, and processed for visualization. All antibodies used were purchased from Santa Cruz Biotechnology (c-fos: sc-52-g; c-jun:sc-44-g; GABP- $\alpha$ : sc-22810-g; Santa Cruz).

**PKC Inhibitors.** NIH-3T3 and COS-7 cells were preincubated with the PKC-specific inhibitors bisindolylmaleimide or RO 32-0432 (Calbiochem, Gibbstown, NJ) for 30 min prior to PMA treatment (50 nM). Twenty-four hours later, promoter activity was measured using the dual luciferase assay as described above. Data were normalized to activity in the untreated control. MA-10 cells were treated with RO 32-0432, PKC $\epsilon$ -specific translocation inhibitor peptide (EAVSLKPT) (Calbiochem), or scrambled peptide (LSETKPAV) (Calbiochem) for 24 h before measuring luciferase activity.

**PKC $\epsilon$  siRNA.** MA-10 cells were seeded at a density of  $4 \times 10^4$ /well in 24-well plates. Cells were transfected 24 h later with 0.2, 0.5, or 2  $\mu$ g of PKC $\epsilon$  siRNA pool of four oligonucleotides (Dharmacon, Lafayette, CO) using X-treme GENE siRNA transfection reagent (Roche) using conditions recommended by the manufacturer. Cells were maintained for 48 h before being harvested for immunoblot analysis performed as described above.

**PKC $\epsilon$  Overexpression.** The pCMV6-XL4 expression plasmid containing *Homo sapiens* protein kinase C, epsilon

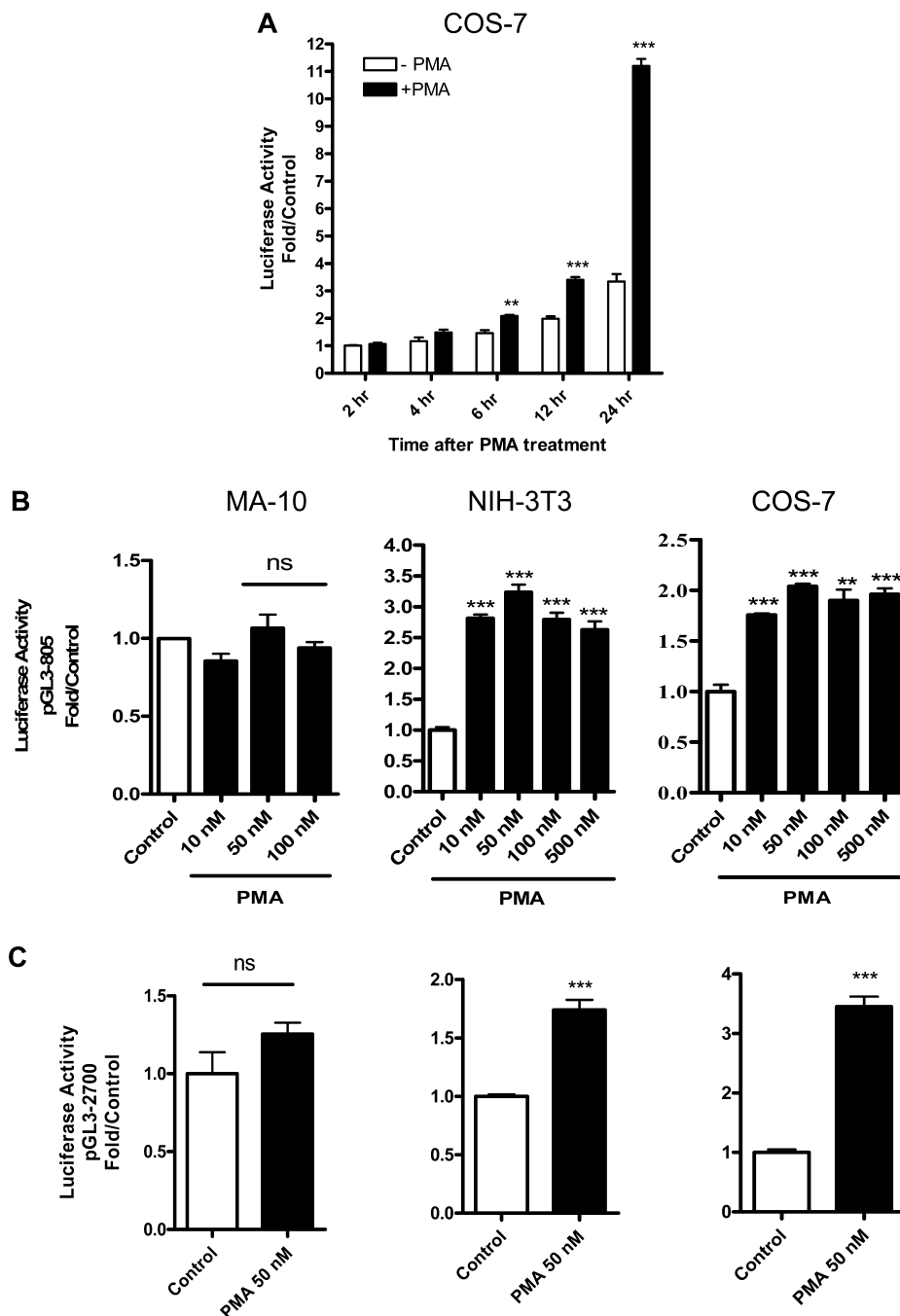


FIGURE 2: Time-dependent induction of *Tspo* promoter activity by PMA. (A) Effect of PMA (50 nM) or DMSO (control) on pGL3-805 luciferase activity in COS-7 cells. (B) Dose-dependent effect of PMA on pGL3-805 luciferase activity in MA-10, NIH-3T3, and COS-7 cells. (C) Effect of PMA (50 nM) on pGL3-2700 luciferase activity in MA-10, NIH-3T3, and COS-7 cells. In B and C, cells were treated with PMA for 24 h. Values are derived from three independent experiments ( $n = 9$ ). \*\* $p < 0.01$  and \*\*\* $p < 0.001$  vs control; ns, nonsignificant.

(PRKCE) was obtained from Origene (Rockville, MD). The plasmid was amplified and purified, and the PKC $\epsilon$  insert was sequenced. The plasmid or empty vector as a control were then transfected into NIH-3T3 cells as described above. Twenty-four hours later, the cells were lysed for mRNA or protein studies. Immunofluorescence using anti-PKC $\epsilon$  antibodies indicated that PKC $\epsilon$  transfection efficiency was approximately 30% (data not shown).

**Sequence and Statistical Analysis.** Sequence analysis was performed using a Vector NTI software (Informax, Invitrogen). Statistical analysis was performed using Prism version 4.0 (GraphPad Software, San Diego, CA). Group means were

compared using student's  $t$  test or two-way ANOVA test followed by a Bonferroni column test. Data are presented as mean  $\pm$  SEM.  $p < 0.05$  was considered significant.

## RESULTS

**TSPO Levels Are Higher in Steroidogenic than Non-steroidogenic Cells.** TSPO binds both the drug ligand, PK 11195, and cholesterol with nanomolar affinities (27). PK 11195 is the most common diagnostic probe for assessing TSPO levels in cellular systems. PK 11195 radioligand binding assays revealed that there were no significant changes in the  $K_d$ , ranging 1–2.5 nM. However, TSPO levels ( $B_{max}$ )



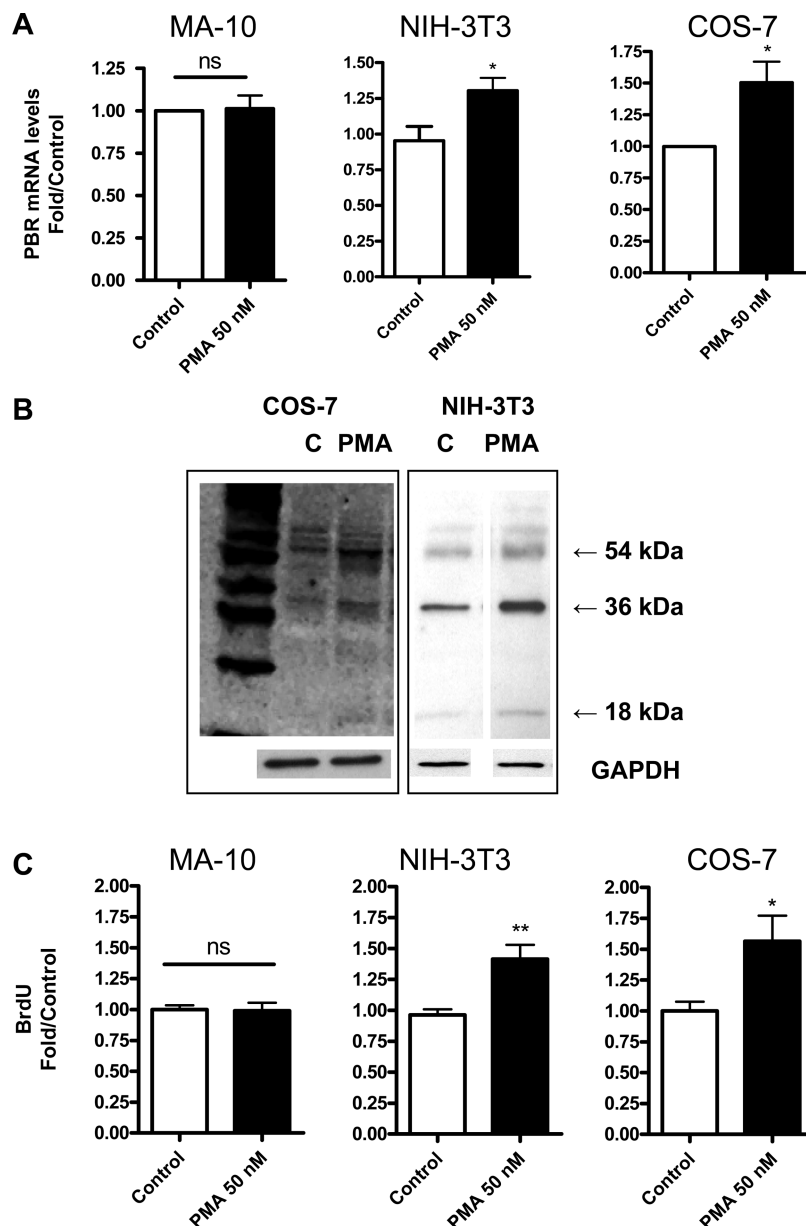


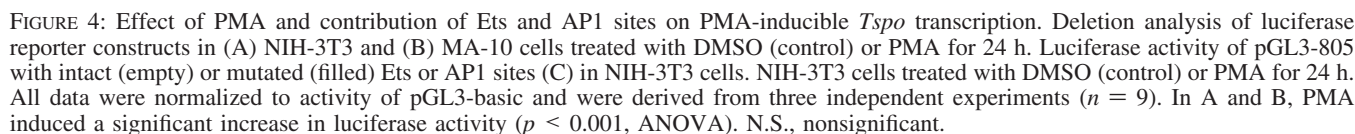
FIGURE 3: PMA induces TSPO mRNA levels, protein levels, and proliferation in NIH-3T3 and COS-7 cells. (A) QRT-PCR analysis of *Tspo* mRNA levels 24 h after PMA treatment. (B) Immunoblot analysis of NIH-3T3 and COS-7 cells treated with and without PMA (50 nM) for 24 h. (C) Cellular BrdU incorporation 24 h after PMA treatment. Results are derived from three independent experiments ( $n = 9$ ). \* $p < 0.05$  and \*\* $p < 0.01$  vs control; ns, nonsignificant. Immunoblots (B) are representative of three independent experiments.

were approximately 10- and 40-fold greater in steroidogenic MA-10 cells than in nonsteroidogenic NIH-3T3 and COS-7 cells, respectively (Figure 1A). Immunoblot analysis confirmed these radioligand binding assay results (Figure 1B). The 18-kDa TSPO protein as well as various putative TSPO homopolymers were detected by immunoblotting as previously reported (27).

**PMA Differentially Regulates *Tspo* Gene Promoter Activity in TSPO-Rich and -Poor Cells.** To explore the regulatory mechanisms underlying differential TSPO expression in various cell models, we tested the effect of PMA on *Tspo* promoter activity in TSPO-rich MA-10 and TSPO-poor NIH-3T3 and COS-7 cells. In COS-7 cells transfected with a luciferase reporter containing 805 bp of the mouse *Tspo* promoter (pGL3-805), exposure to 50 nM PMA resulted in a progressive increase in luciferase activity (Figure 2A). Maximal *Tspo* promoter activity occurred 24 h after PMA

exposure and was at least 2.5-fold greater than activity in the untreated DMSO control. No additional increases in *Tspo* promoter activity were observed beyond 24 h (data not shown). Next, we determined the concentration of PMA needed to induce maximal pGL3-805 activity at 24 h in MA-10, NIH-3T3, and COS-7 cells. PMA elicited maximal activity in NIH-3T3 cells (3.5-fold) and COS-7 cells (2.5-fold) when used at a concentration of 50 nM (Figure 2B). In contrast, none of the PMA concentrations tested increased *Tspo* promoter activity in MA-10 cells, which expressed the highest levels of TSPO (Figure 2B). Promoter activity remained unresponsive to PMA after extending the incubation time to 48 h (data not shown). On the basis of the results from these initial two experiments, cells were treated with 50 nM PMA for 24 h in all subsequent studies.

To investigate whether PMA differentially regulates the full-length mouse *Tspo* promoter (2700 bp) as it does the



**PMA Differentially Regulates *Tspo* mRNA and Protein Levels in TSPO-Rich and -Poor Cells.** PMA did not alter *Tspo* mRNA levels in MA-10 cells either at 24 h (Figure 3A) or 48 h (data not shown). In contrast, a 24 h treatment with PMA increased *Tspo* mRNA levels by approximately 1.25-fold in NIH-3T3 cells and 1.5-fold in COS-7 cells (Figure 3A). In both NIH-3T3 and COS-7 cells, this induction of *Tspo* mRNA levels was accompanied by increases in TSPO protein levels (Figure 3B) and BrdU incorporation (Figure 3C). Densitometric analysis of the gels compared to control GAPDH indicated that the increase in the 18-kDa TSPO and the 36- and 54-kDa polymers was 1.5-fold in COS-7 cells and over 2-fold in NIH-3T3 cells.

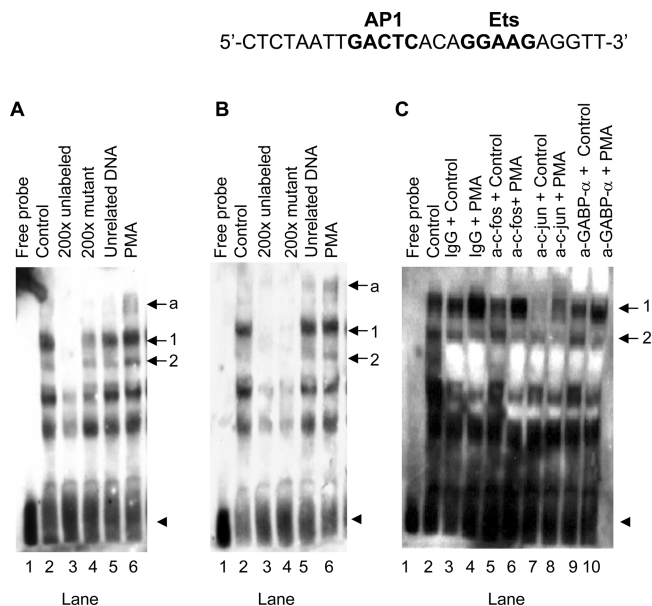


**FIGURE 5:** PMA induces *c-fos*, *c-jun*, and GABP- $\alpha$  binding to their putative binding sites on the *Tspo* promoter. (A and B) EMSA of biotinylated AP1 oligonucleotide incubated without (A and B, lane 1) or with NIH-3T3 nuclear extract (A and B, lane 2). Competition experiments were performed using unlabeled AP1 oligonucleotide (A and B, lane 3), AP1 mutant oligonucleotide (A, lane 4), Ets mutant oligonucleotide (B, lane 4), or unrelated oligonucleotide (A and B, lane 5). The effect of PMA on the formation of DNA–protein complexes is shown in lane 6 (A and B). Arrows 1 and 2 indicate specific complexes, and the arrow labeled ‘a’ indicates a PMA-induced DNA–protein complex. The free probe is indicated with an arrowhead. (C) Supershift/ immunodepletion analysis. EMSAs were performed on nuclear extracts from NIH-3T3 cells treated without (lanes 3, 5, 7, 9) and with PMA (lanes 4, 6, 8, 10). Binding reactions were performed in the presence of IgG (lanes 3 and 4), *c-fos* antibody (lanes 5 and 6), *c-jun* antibody (lanes 7 and 8), or GABP- $\alpha$  antibody (lanes 9 and 10). DNA–protein binding was optimized by including 10  $\mu$ g of BSA and 4 mM DTT in the binding reactions. Results shown are representative of three independent experiments.

In MA-10 cells, PMA did not affect TSPO levels (data not shown) and BrdU incorporation.

**Putative AP1 and Ets Binding Sites in the Proximal Promoter Are Strong Positive Elements Regulating *Tspo* Expression.** To measure the activity of cis-acting elements and to localize the effect of PMA on the mouse promoter, we transiently transfected MA-10, NIH-3T3, and COS-7 cells with reporter constructs containing sequential unidirectional deletions in the 2700-bp mouse *Tspo* promoter (5). In NIH-3T3 cells, the 805-bp fragment was necessary to support full basal activity (Figure 4A). PMA treatment increased activity of the 805 bp-promoter by 3-fold in these cells (Figure 4A). In MA-10 cells (Figure 4B), the 585-bp fragment was the smallest fragment able to support full basal promoter activity. In these cells, all lengths of the *Tspo* promoter were unresponsive to PMA treatment (Figure 4B). Nevertheless, the basal activity of the full-length promoter in MA-10 cells was double that in NIH-3T3 cells. In NIH-3T3 cells, the 805-bp promoter had a 2-fold greater activity than the 2700-bp promoter, suggesting that putative inhibitory elements in the 2700–805 bp promoter region are engaged in NIH-3T3 cells (Figure 4A). Importantly, the effect of PMA was significantly reduced when the 585–515-bp promoter areas were deleted in NIH-3T3 cells. Results obtained using COS-7 cells in general parallel those seen with NIH 3T3 cells (data not

shown). However, because the monkey *Tspo* promoter has not yet been isolated and characterized, detailed studies on the regulation of the mouse *Tspo* promoter in monkey kidney COS-7 cells cannot be interpreted correctly and thus not presented herein.

These results imply that the promoter region spanning from 805 to 515 bp contains cis-acting regulatory elements that drive *Tspo* expression in response to PMA. Analysis of the 805–515 bp region for putative transcription binding sites revealed the presence of two putative Ets binding sites and one AP1 putative binding site. To determine if these sites may regulate *Tspo* expression, we constructed luciferase reporter constructs containing point mutations in these promoter sites. In NIH-3T3 cells, mutation of the first Ets site did not appreciably affect promoter activation by PMA (Figure 4C). Mutation of the second Ets site or the AP1 site reduced PMA-induced promoter activity.

**PMA Induces Binding of *c-Fos*, *c-Jun*, and GABP- $\alpha$  to *Tspo* Promoter Sequences.** EMSA was performed to investigate the effect of PMA on protein interactions at the AP1 and Ets sites suspected to mediate the PMA effect on *Tspo* promoter regulation (Figure 4C). It is of importance to mention that the AP1 and Ets sites are separated by 3 bp only leading to identical wild-type and labeled probes, referred to as the AP1 oligonucleotide. Incubation of NIH-3T3 nuclear extracts with labeled AP1 oligonucleotide (Table 1) generated two specific complexes (Figure 5A and B, lane 2 for both, arrows 1 and 2). The specificity of these interactions was confirmed by the addition of 200-fold excess of unlabeled AP1 oligonucleotide, which competed the formation of the complexes (Figure 5A and B, lane 3) or unrelated oligonucleotide (Epstein–Barr virus nuclear antigen recognition site, lane 5). The addition of a 200-fold excess of unlabeled oligonucleotide carrying a mutation on the putative AP1 site decreased the formation of both DNA–protein complexes (Figure 5A, lane 4). On the other hand, a mutated Ets binding sequence (Figure 5B, lane 4) successfully competed for nuclear proteins in both complexes. The Ets mutated site was more effective than the AP1 mutated site in decreasing the formation of these complexes. PMA treatment resulted in an increase of complexes 1, 2, and the induction of complex ‘a’ (Figure 5A and B, compare lanes 6 and 2).

To obtain the best conditions for binding of the transcription factors to the DNA the experimental conditions were modified (data not shown). Addition of 10  $\mu$ g of BSA and 4 mM DTT in the incubation buffer improved the DNA–protein binding (Figure 5C). Under these conditions, the same two DNA–protein complexes were observed (Figure 5C, lane 2). To identify the proteins bound to the sequence, we performed supershift/ immunodepletion analysis. Addition of *c-fos* antibody (Figure 5C, lane 5), *c-jun* antibody (lane 7), or GABP- $\alpha$  antibody (lane 9), but not nonspecific IgG (lane 3), reduced basal nuclear protein binding to DNA in complex 1. In agreement with data shown in Figure 5A and B, PMA treatment induced the formation of complex 1 (Figure 5C, lane 4). This increase was also reduced in presence of *c-fos* antibody (lane 6), GABP- $\alpha$  antibody (lane 10), or *c-jun* antibody (lane 8). In the later case, complexes 1 and 2 almost completely disappeared (Figure 5C, lane 8). Complex 2 was reduced in presence of *c-fos* antibody (lane 6) and GABP- $\alpha$  antibody (lane 10).

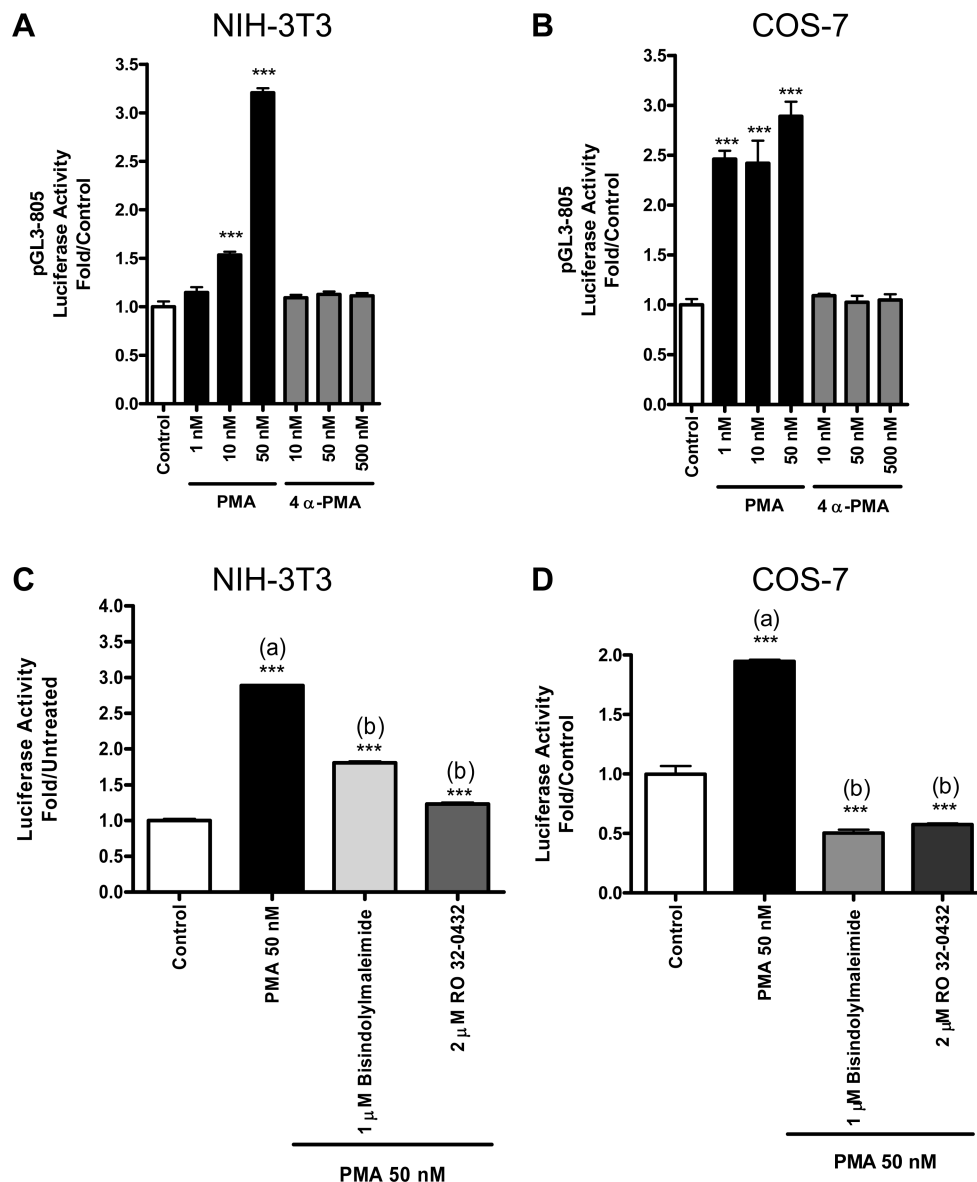


FIGURE 6: PMA induction of the *Tspo* promoter is PKC-dependent. Luciferase activity of pGL3-805 in NIH-3T3 (A) and COS-7 (B) cells treated with DMSO (control-white bars), PMA (black bars), or 4 $\alpha$ -PMA (gray bars) for 24 h. Effect of PKC-specific inhibitors on PMA-inducible pGL3-805 activity in NIH-3T3 (C) and COS-7 (D) cells. In A–D, data were normalized to control activity and were derived from three independent experiments ( $n = 9$ ). \*\*\* $p < 0.001$  vs control.

**PMA Induction of *Tspo* Promoter Activity Is PKC-Dependent.** Since PMA is a PKC activator, we investigated whether PKC mediates induction of the *Tspo* promoter by PMA. To do this, we measured *Tspo* promoter activity in the presence of 4 $\alpha$ -PMA, an inactive structural analog of PMA. PMA induced a dose-dependent induction of *Tspo* promoter activity in NIH-3T3 cells; 50nM PMA elicited a maximal (3-fold) effect (Figure 6A). Under the same conditions, 4 $\alpha$ -PM failed to affect promoter activity, even when used at a 10-times greater concentration (Figure 6A). Similar results were obtained using COS-7 cells (Figure 6B). To confirm this finding, we tested the effect of PKC-specific inhibitors (i.e., bisindolylmaleimide and RO 32-0432) on PMA induction of *Tspo* promoter activity in NIH-3T3 and COS-7 cells. Both inhibitors reduced or abolished the effect of PMA in both NIH-3T3 and COS-7 cells (Figure 6C and D).

**TSPO-Rich MA-10 Cells Express High Levels of PKC $\epsilon$ .** A dose–response study of the effect of RO 32-0432 on

PMA-induced *Tspo* promoter activity in NIH-3T3 cells revealed that this compound was able to inhibit in a dose-dependent manner the PMA effect (Figure 7A). RO 32-0432 exhibits selectivity in its inhibition of PKC $\alpha$  (IC<sub>50</sub> = 9 nM), PKC $\beta$ I (IC<sub>50</sub> = 28 nM), and PKC $\epsilon$  (IC<sub>50</sub> = 180 nM) (28). In the dose–response study, only the highest concentrations of RO 32-0432 were able to abolish the effect of PMA, suggesting that PKC $\epsilon$  mediates the effects of PMA. Immunoblot analysis of PKC isoforms in MA-10, NIH-3T3, and COS-7 cells revealed that each cell line differentially expressed the PKC $\alpha$ , PKC $\beta$ II, and PKC $\epsilon$  isoforms. PKC $\alpha$  was highly expressed in NIH-3T3 cells compared to MA-10 cells (Figure 7B). On the other hand, PKC $\beta$ II and PKC $\epsilon$  were more highly expressed in MA-10 cells than in NIH-3T3 and COS-7 cells.

**Inhibition of PKC $\epsilon$  Reduces Basal *Tspo* Promoter Activity in TSPO-Rich MA-10 Cells and PKC $\epsilon$  siRNA Lowers PKC $\epsilon$  and TSPO Protein Levels.** As noted earlier, PMA does not affect *Tspo* expression in MA-10 cells and basal *Tspo*



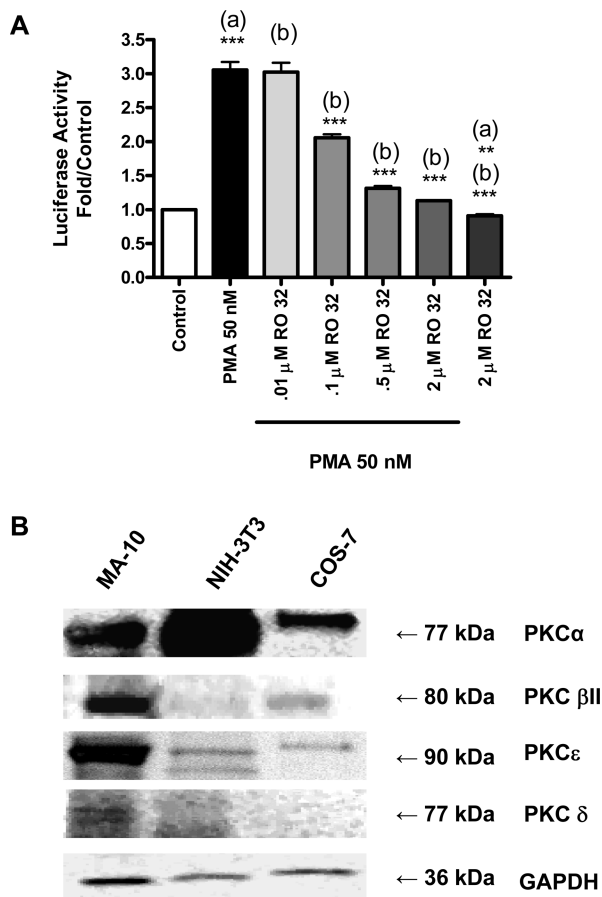


FIGURE 7: *Tspo* promoter sensitivity to RO 32-0432 and PKC isoform expression. (A) Dose-dependent effect of RO 32-0432 on pGL3-805 activity in NIH-3T3 cells. Results are derived from three independent experiments ( $n = 9$ ).  $^{**}p < 0.01$  and  $^{***}p < 0.001$  vs (a) control, (b) PMA. (B) Immunoblot analysis of PKC isoforms in MA-10, NIH-3T3, and COS-7 cells. The blots shown are representative of two independent experiments.

promoter activity in these cells is 2-fold higher than in NIH-3T3 and COS-7 cells. To determine if PKC regulates *Tspo* promoter activity in MA-10 cells, we measured promoter activity in the presence of calphostin, RO 32-0432, or G06976. Calphostin inhibits PKC $\alpha$ , PKC $\beta$ , and with variable efficacy, PKC $\epsilon$ . On the other hand, G06976 inhibits PKC $\alpha$  and PKC $\beta$  but does not affect PKC $\epsilon$ , even at micromolar concentrations while as mentioned above RO 32-0432 exhibits selectivity in its inhibition of the conventional subtypes PKC $\alpha$ , PKC $\beta$ , and the unconventional subtype PKC $\epsilon$  (28, 29). Neither calphostin nor G06976 inhibited *Tspo* promoter activity, whereas RO 32-0432 (2  $\mu$ M) reduced basal promoter activity by 40% (Figure 8A). In accord with this finding, a PKC $\epsilon$ -specific translocation inhibitor peptide inhibited basal *Tspo* promoter activity by 50% (Figure 8B). This effect was absent in cells treated with scrambled peptide. The RO 32-0432-induced reduction in basal promoter activity was accompanied by a decrease in BrdU incorporation (Figure 8C). Importantly, concentrations of RO 32-0432 expected to inhibit PKC $\epsilon$  activity, abolished BrdU incorporation.

To confirm these findings on the putative role of PKC $\epsilon$  in the regulation of *Tspo* gene expression, PKC $\epsilon$  siRNA was used to lower PKC $\epsilon$  protein levels in TSPO-rich MA-10 cells. Figure 8D shows that the PKC $\epsilon$  siRNA pool used inhibited in a dose-dependent PKC $\epsilon$  protein expression reaching a 70% inhibition in the presence of 2  $\mu$ g of siRNA. Under the same

conditions, the siRNA used also induced a dose-dependent reduction in TSPO protein levels (Figure 8D). GAPDH and PKC $\alpha$  levels remained unchanged.

**PKC $\epsilon$  Overexpression in NIH-3T3 Cells Up Regulates *Tspo* Promoter Activity, mRNA and Protein Levels, and Potentiates the Effect of PMA.** In an effort to further evaluate the role of PKC $\epsilon$  in the regulation of *Tspo* expression, we tested the impact of PKC $\epsilon$  overexpression on TSPO levels in the TSPO-poor NIH-3T3 cells. Expression of exogenous PKC $\epsilon$  was confirmed by immunoblot analysis (Figure 9A). These data also show that PKC $\epsilon$  was not degraded in response to the PMA treatment. A time course treatment of NIH-3T3 and COS-7 cells with PMA indicated that PKC $\epsilon$  levels were the same in control and treated cells for times as long as 10 h, suggesting that this enzyme is resistant to degradation (data not shown). Transfecting NIH-3T3 cells with the wild-type PKC $\epsilon$  significantly induced the pGL3-805 *Tspo* promoter activity and treatment with PMA further induced the effect (Figure 9B). Under the same conditions, there was no induction in *Tspo* promoter activity using a promoter where AP1 was mutated, suggesting that the effect seen is likely mediated through this AP1 site. No significant difference was observed in the pGL3-basic in response to PKC $\epsilon$  overexpression. PMA induced both *Tspo* mRNA and protein levels to a greater degree in PKC $\epsilon$ -overexpressing cells than in control cells (Figure 9C-E).

**PKC $\epsilon$  Overexpression in NIH-3T3 Cells Induces c-Jun Protein Transcription and Phosphorylation.** Because PMA induced binding of c-jun to a *Tspo* promoter sequence (Figure 5C), we also examined the effect of PKC $\epsilon$  overexpression on c-jun protein levels and phosphorylation (Ser73). PMA induced c-jun levels by 2-fold in control cells and over 6-fold in PKC $\epsilon$ -overexpressing cells (Figure 10A and B). Normalizing the levels of phosphorylated c-jun to GAPDH and dividing them by the c-jun levels indicates that a large portion of PMA inducible c-jun underwent phosphorylation in the PKC $\epsilon$ -overexpressing cells (Figure 10C and D).

## DISCUSSION

Here, we provide evidence that *Tspo* promoter activity and expression are regulated by a PKC $\epsilon$ -dependent signaling pathway in steroidogenic and nonsteroidogenic cells. This is the first report clearly linking induction of *Tspo* expression to a signal transduction pathway. In this study, we investigated the molecular mechanisms governing *Tspo* regulation by exploring *Tspo* transcriptional responses to a tumor-promoting agent in the three cell lines with varying TSPO levels. Our data clearly showed that only nonsteroidogenic cells expressing low levels of TSPO (i.e., NIH-3T3 and COS-7 cells) responded to PMA, as seen by an increase in *Tspo* promoter activity, *Tspo* mRNA and protein levels, and cellular proliferation. MA-10 cells are rapidly dividing, aggressive tumor cells, so further induction of proliferation with PMA may not be possible. The finding that basal *Tspo* activity was significantly higher in MA-10 cells than in NIH-3T3 or COS-7 cells suggests that an endogenous factor linked to the steroidogenic phenotype of the MA-10 cells drives the constitutive *Tspo* expression in these cells.

Sequence analysis of the *Tspo* promoter region crucial for *Tspo* induction in PMA-treated NIH-3T3 cells revealed the presence of two Ets sites and one AP1 site. Members of both

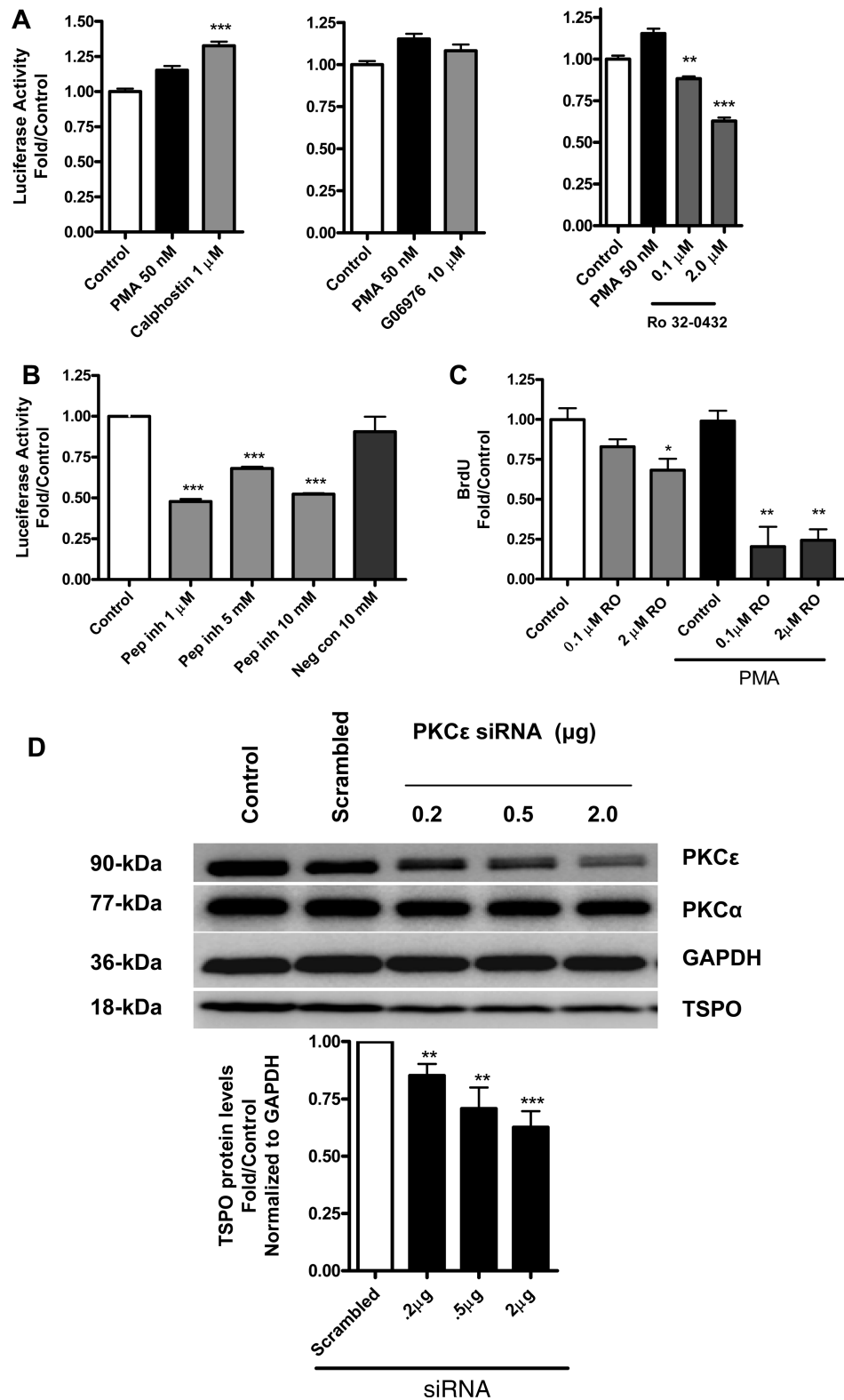


FIGURE 8: PKCε mediates PMA-induced *Tspo* promoter activity and TSPO protein levels. (A) Effect of calphostin, G06976, or RO 32-0432 on PMA-inducible pGL3-805 activity in MA-10 cells. (B) Effect of a PKCε-specific translocation inhibitor peptide (Pep Inh) or scrambled peptide (Neg Con) on PMA-inducible pGL3-805 activity. (C) Effect of RO 32-0432 on PMA-induced MA-10 proliferation. (D) Effect of down regulation of PKCε on TSPO protein levels. Cells were treated with the siRNA pool specific for PKCε or scrambled oligonucleotides as described under materials and methods. At the end of the experiment, cells were analyzed for PKCε, PKCα, TSPO, and GAPDH expression by immunoblot analysis. Results for A–C are derived from three independent experiments ( $n = 9$ ). \* $p < 0.05$ , \*\* $p < 0.01$ , and \*\*\* $p < 0.001$  vs control. Immunoblots (D) are representative of two independent experiments.

AP1 and Ets transcription factor families are known to bind to the *Tspo* promoter (5, 14). These transcription factors can regulate transcription either alone, in cooperation with each other, or in cooperation with different transcription factors

or cofactors. Deletion analysis revealed that only the second Ets site and its adjacent AP1 site contributed to promoter induction by PMA in NIH-3T3 cells. An additive effect was not observed upon mutation of both sites, suggesting that

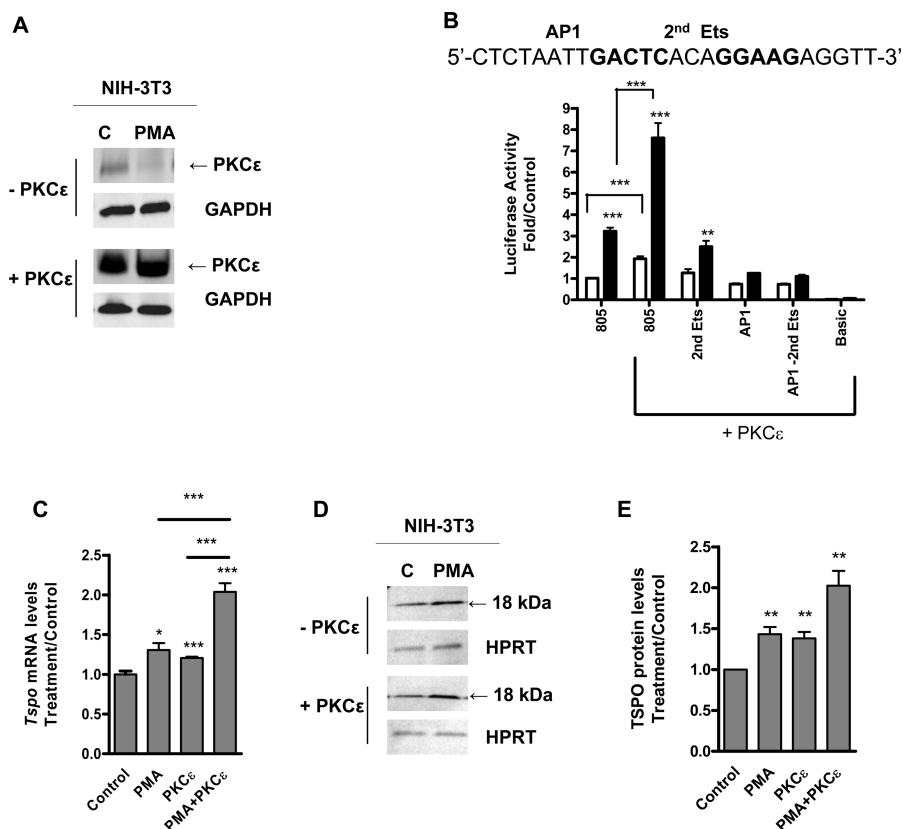


FIGURE 9: PKC $\epsilon$  overexpression induces *Tspo* promoter mRNA and protein levels. NIH-3T3 cells were transfected with PKC $\epsilon$  expression vector or vector only, then treated with (white bars) or without PMA (black bars) for 24 h. (A) Immunoblot analysis of cell extracts. (B) Effect of PKC $\epsilon$  overexpression on *Tspo* promoter activity. (C) QRT-PCR analysis of *Tspo* mRNA levels in response to PKC $\epsilon$  overexpression. Results are derived from three independent experiments ( $n = 9$ ). \* $p < 0.05$ , \*\* $p < 0.01$ , and \*\*\* $p < 0.001$  vs control. (D) Immunoblot analysis of TSPO and (E) densitometry of TSPO bands. Immunoreactive bands were normalized to HPRT, and these values were expressed as an increase relative to control. Immunoblots are representative of three independent experiments.

one of the two sites is used at a time. This idea is consistent with the close proximity of the Ets and AP1 sites (separated by 3 bp), which would make simultaneous occupancy of the same site difficult due to allosteric hindrance. In TSPO-rich MA-10 cells, mutation of the AP1 site or either of the two Ets sites did not restore the ability of the *Tspo* gene promoter to respond to PMA (data not shown), suggesting that additional increases in the basal promoter activity of these cells is not possible.

EMSA of NIH-3T3 extracts revealed that c-jun and c-fos (of the AP1 family) as well as GABP- $\alpha$  (of the Ets family) bound to the AP1 site of the *Tspo* promoter in a PMA-inducible manner. In these studies, we observed that a mutation of the Ets site was more successful at competing off specific complexes 1 and 2 (Figure 5B, lane 4). It is possible that some AP1 factors maybe bound to the AP1 site thus preventing the probe from accessing the DNA. Mutating the AP1 site prevented this binding, and thus, the complexes formed were not competed. This is supported by the fact that c-jun almost completely disrupted the probe binding (Figure 5C, lanes 7 and 8). These findings suggest that PMA induces either synthesis of these transcription factors or their binding to DNA through the activation of a signal transduction pathway, such as the PKC pathway. In TSPO-rich cells, such as MA-10 cells, PKC might maintain constitutive *Tspo* promoter activity by modulating the phosphorylation state and activity of transcription factors, such as AP1 family members, or other regulatory proteins (30). In TSPO-poor cells, PMA induces c-jun, c-fos, and

GABP- $\alpha$  transcription and DNA binding, acting probably via PKC. The interaction of these transcription factors with the *Tspo* promoter was recently confirmed by chromatin immunoprecipitation assays (14).

In recent years, PKC has been linked to multiple diseases, steroidogenesis, and cancers (31–33). PKC mediates the tumor-promoting effects of PMA, although PMA is also known to have PKC-independent effects (34). The ability of PKC-specific inhibitors to abrogate PMA-induced promoter activity, taken with the inability of 4 $\alpha$ -PMA to induce promoter activity, suggests that PMA acts through PKC to induce *Tspo* transcription. Different PKC isoforms may regulate *Tspo* transcription in COS-7 and NIH-3T3 cells, since these cells had different inhibition profiles. Alternatively, conventional and nonconventional PKC isoforms may cooperatively regulate transcription in these cells. The finding that bisindolylmaleimide and RO 32-0432 inhibited the inducible effect of PMA in NIH-3T3 cells is consistent with a role for PKC $\epsilon$  in PMA-activated *Tspo* transcription. The ability of RO 32-0432 to abolish PMA-induced promoter activity only at concentrations found to inhibit PKC $\epsilon$  also supports this idea.

Our findings pointed to a role for PKC $\epsilon$  not only in inducing *Tspo* expression in NIH-3T3 and COS-7 cells but also in basal *Tspo* expression in MA-10 cells. Of the three cell lines examined, MA-10 cells had the highest expression of PKC $\epsilon$ . In addition, basal constitutive *Tspo* promoter activity in MA-10 cells was decreased, not by calphostin or G06976, but by a high enough dose of RO 32-0432 to affect

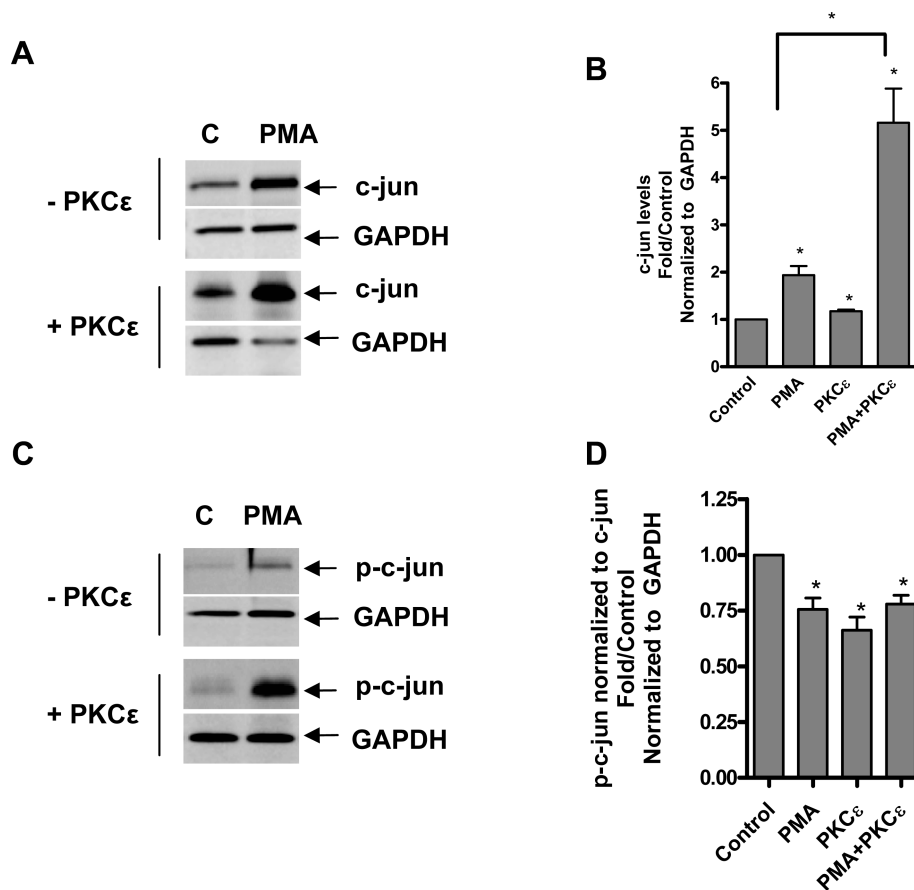


FIGURE 10: PKC $\epsilon$  overexpression induces c-jun protein levels and phosphorylation. NIH-3T3 cells were transfected with PKC $\epsilon$  expression vector or vector only, then treated with or without PMA for 24 h and examined for c-jun levels by immunoblotting (A) followed by densitometric (B) analysis of the blots. Immunoreactive bands were normalized to GAPDH, and these values were expressed as an increase relative to control. Immunoblot (C) and densitometric (D) analysis of phosphorylated c-jun (Ser73). p-c-Jun levels were normalized to GAPDH levels (data not shown), then normalized to c-jun levels to investigate phosphorylation of newly synthesized protein. Immunoblots are representative of two independent experiments.

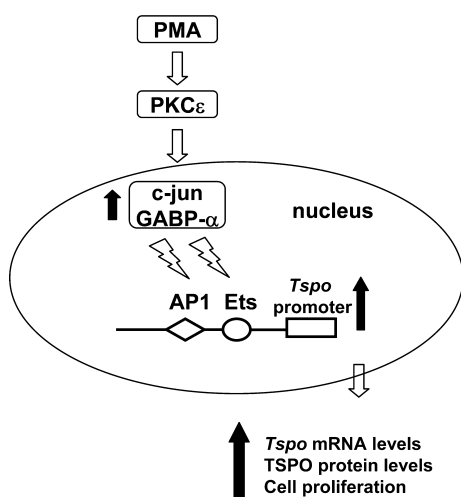


FIGURE 11: Proposed signaling pathway underlying PMA-induced activation of the *Tspo* promoter.

PKC $\epsilon$ . Similar inhibition was observed in the presence of a specific PKC $\epsilon$  translocation inhibitor peptide, which prevents the translocation of PKC $\epsilon$  to its anchoring protein (19). Moreover, lowering PKC $\epsilon$  protein levels following siRNA treatment of MA-10 cells was accompanied by a reduction in TSPO protein levels. The finding that, under the conditions used, 70% reduction in PKC $\epsilon$  protein levels led to 40% reduction in TSPO suggests that either longer periods of

incubation time with the siRNA used are needed to deplete the endogenous TSPO or that other mechanisms account for the control of the remaining TSPO expression. Taken together, these data indicate that PKC $\epsilon$  is an important component of the basal transcription of *Tspo* in TSPO-rich steroidogenic MA-10 cells.

PKC $\epsilon$  is a crucial player in diabetes (35) and Alzheimer's disease (36). It is also involved in carcinogenesis (23, 37–39) and participates in tumor development, metastasis, and invasion in many tissues. Overexpression of PKC $\epsilon$  confers oncogenic potential to fibroblasts, colonic, and prostatic epithelial cells (40, 41). In addition, high-grade tumors frequently have high levels of PKC $\epsilon$  (23, 31, 42). Diminishing high levels or activity of PKC $\epsilon$  may suppress tumor promotion, growth, invasiveness, and metastasis (39). For example, PKC $\epsilon$  inhibition reduces tumor growth and metastasis of MDA-MB-231 breast cancer cells (42) and sensitizes breast cancer cells to tumor necrosis factor-induced death (43). Interestingly, the profile of TSPO expression in Alzheimer's disease (4) and various cancers (1, 6–10) as well as the role of TSPO in cell proliferation, tumor invasion, and tumor metastasis (1, 6, 11, 44) parallels that of PKC $\epsilon$ . Considering that TSPO controls the rate of adrenal cortical steroid formation (45) and this shared profile between PKC $\epsilon$  and TSPO, it is not surprising that PKC $\epsilon$  null mice have dramatically reduced circulating corticosterone levels (46).



Indeed, this phenotype may be attributable to reduced adrenal cortical levels of TSPO.

The importance of PKC $\epsilon$  on *Tspo* promoter activity was confirmed through overexpression of PKC $\epsilon$  in NIH-3T3 cells, which expressed low levels of this PKC isoform as well as of TSPO. Although prolonged exposure to PMA has been reported to degrade PKC (47), we found that, in these cells, PKC $\epsilon$  was resistant to PMA degradation, in agreement with previous reports on this isoform (48), thus ruling out the possibility that the PMA effect might be due to PKC $\epsilon$  degradation following prolonged exposure to PMA. Also in agreement with previous findings (49), PKC $\epsilon$  overexpression increased NIH-3T3 proliferation (data not shown). Importantly, although PKC $\epsilon$  overexpression increased *Tspo* mRNA and protein levels, PMA greatly enhanced this effect. Thus, PKC $\epsilon$  is essential for *Tspo* gene expression but must be activated to exert this effect.

The results presented here suggest that, in TSPO-rich steroidogenic cells, constitutive expression of high levels of PKC $\epsilon$  drives *Tspo* expression. In TSPO-poor nonsteroidogenic cells, this pathway can be engaged by tumor-promoting agents, also resulting in increased proliferation. In the TSPO-poor NIH-3T3 cell line, PMA induced *Tspo* transcription primarily through the formation of c-jun DNA binding complexes and to a lesser extent GABP- $\alpha$  complexes. The finding that PMA treatment of NIH-3T3 cells elicited a dramatic up regulation of c-jun in the presence of PKC $\epsilon$  overexpression provides further support for the PKC $\epsilon$ →c-jun→*Tspo* signaling axis (Figure 11). In PKC $\epsilon$ -transfected NIH-3T3 cells, a large fraction of PMA-induced c-jun was phosphorylated. These data further indicate that PMA treatment induces both c-jun expression and activity, which drives *Tspo* expression.

In summary, a PKC $\epsilon$ -dependent signal transduction pathway drives *Tspo* transcription and expression through activation of AP1 and Ets transcription factors. This is the first clear evidence linking increased TSPO expression to a signal transduction pathway (PKC $\epsilon$ ). Additional studies will be necessary to unravel the exact mechanism by which PKC $\epsilon$  regulates AP1 and Ets expression and/or activity.

## REFERENCES

- Papadopoulos, V., Baraldi, M., Guilarte, T. R., Knudsen, T. B., Lacapere, J. J., Lindemann, P., Norenberg, M. D., Nutt, D., Weizman, A., Zhang, M. R., and Gavish, M. (2006) Translocator protein (18 kDa): new nomenclature for the peripheral-type benzodiazepine receptor based on its structure and molecular function. *Trends Pharmacol. Sci.* 27, 402–409.
- Braestrup, C., and Squires, R. F. (1977) Specific benzodiazepine receptors in rat brain characterized by high-affinity (3H)diazepam binding. *Proc. Natl. Acad. Sci. U.S.A.* 74, 3805–3809.
- Casellas, P., Galiegue, S., and Basile, A. S. (2002) Peripheral benzodiazepine receptors and mitochondrial function. *Neurochem. Int.* 40, 475–486.
- Gavish, M., Bachman, I., Shoukrun, R., Katz, Y., Veenman, L., Weisinger, G., and Weizman, A. (1999) Enigma of the peripheral benzodiazepine receptor. *Pharmacol. Rev.* 51, 629–650.
- Giatakis, C., and Papadopoulos, V. (2004) Differential utilization of the promoter of peripheral-type benzodiazepine receptor by steroidogenic versus nonsteroidogenic cell lines and the role of Sp1 and Sp3 in the regulation of basal activity. *Endocrinology* 145, 1113–1123.
- Hardwick, M., Fertikh, D., Culty, M., Li, H., Vidic, B., and Papadopoulos, V. (1999) Peripheral-type benzodiazepine receptor (PBR) in human breast cancer: correlation of breast cancer cell aggressive phenotype with PBR expression, nuclear localization, and PBR-mediated cell proliferation and nuclear transport of cholesterol. *Cancer Res.* 59, 831–842.
- Han, Z., Slack, R. S., Li, W., and Papadopoulos, V. (2003) Expression of peripheral benzodiazepine receptor (PBR) in human tumors: relationship to breast, colorectal, and prostate tumor progression. *J. Recept. Signal Transduct. Res.* 23, 225–238.
- Galiegue, S., Casellas, P., Kramar, A., Tinel, N., and Simony-Lafontaine, J. (2004) Immunohistochemical assessment of the peripheral benzodiazepine receptor in breast cancer and its relationship with survival. *Clin. Cancer Res.* 10, 2058–2064.
- Maaser, K., Grabowski, P., Sutter, A. P., Hopfner, M., Foss, H. D., Stein, H., Berger, G., Gavish, M., Zeitz, M., and Scherubl, H. (2002) Overexpression of the peripheral benzodiazepine receptor is a relevant prognostic factor in stage III colorectal cancer. *Clin. Cancer Res.* 8, 3205–3209.
- Katz, Y., Ben-Baruch, G., Kloog, Y., Menczer, J., and Gavish, M. (1990) Increased density of peripheral benzodiazepine-binding sites in ovarian carcinomas as compared with benign ovarian tumours and normal ovaries. *Clin. Sci.* 78, 155–158.
- Veenman, L., Papadopoulos, V., and Gavish, M. (2007) Channel-like functions of the 18-kDa translocator protein (TSPO): regulation of apoptosis and steroidogenesis as part of the host-defense response. *Curr. Pharm. Des.* 13 (23), 2385–405.
- Gazouli, M., Yao, Z. X., Boujrad, N., Corton, J. C., Culty, M., and Papadopoulos, V. (2002) Effect of peroxisome proliferators on Leydig cell peripheral-type benzodiazepine receptor gene expression, hormone-stimulated cholesterol transport, and steroidogenesis: role of the peroxisome proliferator-activator receptor alpha. *Endocrinology* 143, 2571–2583.
- Amri, H., Drieu, K., and Papadopoulos, V. (2003) Transcriptional suppression of the adrenal cortical peripheral-type benzodiazepine receptor gene and inhibition of steroid synthesis by ginkgolide B. *Biochem. Pharmacol.* 65, 717–729.
- Giatakis, C., Batarseh, A., Dettin, L., and Papadopoulos, V. (2007) The role of Ets transcription factors in the basal transcription of the translocator protein (18 kDa). *Biochemistry* 46, 4763–4774.
- Furstenberger, G., Berry, D. L., Sorg, B., and Marks, F. (1981) Skin tumor promotion by phorbol esters is a two-stage process. *Proc. Natl. Acad. Sci. U.S.A.* 78, 7722–7726.
- Saito, N., Kikkawa, U., and Nishizuka, Y. (2002) The family of protein kinase C and membrane lipid mediators. *J. Diabetes Complications* 16, 4–8.
- Nishizuka, Y. (1988) The molecular heterogeneity of protein kinase C and its implications for cellular regulation. *Nature* 334, 661–665.
- Wetsel, W. C., Khan, W. A., Merchenthaler, I., Rivera, H., Halpern, A. E., Phung, H. M., Negro-Vilar, A., and Hannun, Y. A. (1992) Tissue and cellular distribution of the extended family of protein kinase C isoenzymes. *J. Cell Biol.* 117, 121–133.
- da Rocha, A. B., Mans, D. R., Regner, A., and Schwartzmann, G. (2002) Targeting protein kinase C: new therapeutic opportunities against high-grade malignant gliomas? *Oncologist* 7, 17–33.
- Lopez-Ruiz, M. P., Choi, M. S., Rose, M. P., West, A. P., and Cooke, B. A. (1992) Direct effect of arachidonic acid on protein kinase C and LH-stimulated steroidogenesis in rat Leydig cells; evidence for tonic inhibitory control of steroidogenesis by protein kinase C. *Endocrinology* 130 (3), 1122–1130.
- Manna, P. R., Jo, Y., and Stocco, D. M. (2007) Regulation of Leydig cell steroidogenesis by extracellular signal-regulated kinase 1/2: role of protein kinase A and protein kinase C signaling. *J. Endocrinol.* 193 (1), 53–63.
- Jo, Y., King, S. R., Khan, S. A., and Stocco, D. M. (2005) Involvement of protein kinase C and cyclic adenosine 3',5'-monophosphate-dependent kinase in steroidogenic acute regulatory protein expression and steroid biosynthesis in Leydig cells. *Biol. Reprod.* 73 (2), 244–55.
- Griner, E. M., and Kazanietz, M. G. (2007) Protein kinase C and other diacylglycerol effectors in cancer. *Nat. Rev. Cancer* 7, 281–294.
- Ono, Y., Fujii, T., Ogita, K., Kikkawa, U., Igarashi, K., and Nishizuka, Y. (1988) The structure, expression, and properties of additional members of the protein kinase C family. *J. Biol. Chem.* 263, 6927–6932.
- Papadopoulos, V., Amri, H., Li, H., Boujrad, N., Vidic, B., and Garnier, M. (1997) Targeted disruption of the peripheral-type benzodiazepine receptor gene inhibits steroidogenesis in the R2C Leydig tumor cell line. *J. Biol. Chem.* 272, 32129–32135.
- Li, H., Yao, Z., Degenhardt, B., Teper, G., and Papadopoulos, V. (2001) Cholesterol binding at the cholesterol recognition/interac-

- tion amino acid consensus (CRAC) of the peripheral-type benzodiazepine receptor and inhibition of steroidogenesis by an HIV TAT-CRAC peptide. *Proc. Natl. Acad. Sci. U.S.A.* 98, 1267–1272.
27. Delavoie, F., Li, H., Hardwick, M., Robert, J. C., Giatzakis, C., Peranzi, G., Yao, Z. X., Maccario, J., Lacapere, J. J., and Papadopoulos, V. (2003) In vivo and in vitro peripheral-type benzodiazepine receptor polymerization: functional significance in drug ligand and cholesterol binding. *Biochemistry* 42, 4506–4519.
28. Birchall, A. M., Bishop, J., Bradshaw, D., Cline, A., Coffey, J., Elliott, L. H., Gibson, V. M., Greenham, A., Hallam, T. J., and Harris, W. (1994) Ro 32-0432, a selective and orally active inhibitor of protein kinase C prevents T-cell activation. *J. Pharmacol. Exp. Ther.* 268, 922–929.
29. Koyama, N., Kashimata, M., Sakashita, H., Sakagami, H., and Gresik, E. W. (2003) EGF-stimulated signaling by means of PI3K, PLC $\gamma$ 1, and PKC isozymes regulates branching morphogenesis of the fetal mouse submandibular gland. *Dev. Dyn.* 227, 216–226.
30. Gadea, A., Schinelli, S., and Gallo, V. (2008) Endothelin-1 regulates astrocyte proliferation and reactive gliosis via a JNK/c-Jun signaling pathway. *J. Neurosci.* 28, 2394–2408.
31. Fabbro, D., Kung, W., Roos, W., Regazzi, R., and Eppenberger, U. (1986) Epidermal growth factor binding and protein kinase C activities in human breast cancer cell lines: possible quantitative relationship. *Cancer Res.* 46, 2720–2725.
32. Platet, N., Prevostel, C., Derocq, D., Joubert, D., Rochefort, H., and Garcia, M. (1998) Breast cancer cell invasiveness: correlation with protein kinase C activity and differential regulation by phorbol ester in estrogen receptor-positive and -negative cells. *Int. J. Cancer* 75, 750–756.
33. Lahn, M., Sundell, K., Gleave, M., Ladan, F., Su, C., Li, S., Ma, D., Paterson, B. M., and Bumol, T. F. (2004) Protein kinase C- $\alpha$  in prostate cancer. *BJU Int.* 93, 1076–1081.
34. Nakamura, J., Suda, T., Ogawa, Y., Takeo, T., Suga, S., and Wakui, M. (2001) Protein kinase C-dependent and -independent inhibition of Ca<sup>2+</sup> influx by phorbol ester in rat pancreatic beta-cells. *Cell Signal.* 13, 199–205.
35. Ikeda, Y., Olsen, G. S., Ziv, E., Hansen, L. L., Busch, A. K., Hansen, B. F., Shafir, E., and Mosthaf-Seedorf, L. (2001) Cellular mechanism of nutritionally induced insulin resistance in Psammomys obesus: overexpression of protein kinase C epsilon in skeletal muscle precedes the onset of hyperinsulinemia and hyperglycemia. *Diabetes* 50, 584–592.
36. Kinouchi, T., Sorimachi, H., Maruyama, K., Mizuno, K., Ohno, S., Ishiura, S., and Suzuki, K. (1995) Conventional protein kinase C (PKC)- $\alpha$  and novel PKC epsilon, but not -delta, increase the secretion of an N-terminal fragment of Alzheimer's disease amyloid precursor protein from PKC cDNA transfected 3Y1 fibroblasts. *FEBS Lett.* 364, 203–206.
37. Bae, K. M., Wang, H., Jiang, G., Chen, M. G., Lu, L., and Xiao, L. (2007) Protein kinase C epsilon is overexpressed in primary human non-small cell lung cancers and functionally required for proliferation of non-small cell lung cancer cells in a p21/Cip1-dependent manner. *Cancer Res.* 67, 6053–6063.
38. Aziz, M. H., Manoharan, H. T., and Verma, A. K. (2007) Protein kinase C epsilon, which sensitizes skin to sun's UV radiation-induced cutaneous damage and development of squamous cell carcinomas, associates with Stat3. *Cancer Res.* 67, 1385–1394.
39. Pan, Q., Bao, L. W., Teknos, T. N., and Merajver, S. D. (2006) Targeted disruption of protein kinase C  $\epsilon$  reduces cell invasion and motility through inactivation of RhoA and RhoC GTPases in head and neck squamous cell carcinoma. *Cancer Res.* 66, 9379–9384.
40. Perletti, G. P., Concari, P., Brusaferrri, S., Marras, E., Piccinini, F., and Tashjian, A. H. (1998) Protein kinase C epsilon is oncogenic in colon epithelial cells by interaction with the ras signal transduction pathway. *Oncogene* 16, 3345–3348.
41. Wu, D., Foreman, T. L., Gregory, C. W., McJilton, M. A., Wescott, G. G., Ford, O. H., Alvey, R. F., Mohler, J. L., and Terrian, D. M. (2002) Protein kinase epsilon has the potential to advance the recurrence of human prostate cancer. *Cancer Res.* 62, 2423–2429.
42. Pan, Q., Bao, L. W., Kleer, C. G., Sabel, M. S., Griffith, K. A., Teknos, T. N., and Merajver, S. D. (2005) Protein kinase C epsilon is a predictive biomarker of aggressive breast cancer and a validated target for RNA interference anticancer therapy. *Cancer Res.* 65, 8366–8371.
43. Basu, A., Mohanty, S., and Sun, B. (2001) Differential sensitivity of breast cancer cells to tumor necrosis factor- $\alpha$ : involvement of protein kinase C. *Biochem. Biophys. Res. Commun.* 280, 883–891.
44. Li, W., Hardwick, M. J., Rosenthal, D., Culty, M., and Papadopoulos, V. (2007) Peripheral-type benzodiazepine receptor overexpression and knockdown in human breast cancer cells indicate its prominent role in tumor cell proliferation. *Biochem. Pharmacol.* 73, 491–503.
45. Lacapere, J. J., and Papadopoulos, V. (2003) Peripheral-type benzodiazepine receptor: structure and function of a cholesterol-binding protein in steroid and bile acid biosynthesis. *Steroids* 68, 569–585.
46. Hodge, C. W., Raber, J., McMahon, T., Walter, H., Sanchez-Perez, A. M., Olive, M. F., Mehmet, K., Morrow, A. L., and Messing, R. O. (2002) Decreased anxiety-like behavior, reduced stress hormones, and neurosteroid supersensitivity in mice lacking protein kinase Cepsilon. *J. Clin. Invest.* 110, 1003–1010.
47. Hofmann, J. (2001) Modulation of protein kinase C in antitumor treatment. *Rev. Physiol. Biochem. Pharmacol.* 142, 1–96.
48. Cai, H., Smola, U., Wixler, V., Eisenmann-Tappe, I., az-Meco, M. T., Moscat, J., Rapp, U., and Cooper, G. M. (1997) Role of diacylglycerol-regulated protein kinase C isotypes in growth factor activation of the Raf-1 protein kinase. *Mol. Cell. Biol.* 17, 732–741.
49. Mischak, H., Goodnight, J. A., Kolch, W., Martiny-Baron, G., Schaehtle, C., Kazanietz, M. G., Blumberg, P. M., Pierce, J. H., and Mushinski, J. F. (1993) Overexpression of protein kinase C-delta and -epsilon in NIH 3T3 cells induces opposite effects on growth, morphology, anchorage dependence, and tumorigenicity. *J. Biol. Chem.* 268, 6090–6096.

BI8012643